diversity

MDPI

Article

Morphostructural Characterization of the Heterogeneous Rhodolith Bed at the Marine Protected Area "Capo Carbonara" (Italy) and Hydrodynamics

Valentina A. Bracchi [1,2,*], Sarah Caronni [1], Agostino N. Meroni [1], Esteban Gottfried Burguett [1], Fabrizio Atzori [3], Nicoletta Cadoni [3], Fabio Marchese [4] and Daniela Basso [1,2]

1 Department of Earth and Environmental Sciences, University of Milano-Bicocca, 20126 Milan, Italy; sarah.caronni@unimib.it (S.C.); agostino.meroni@unimib.it (A.N.M.); e.gottfriedburgue@campus.unimib.it (E.G.B.); daniela.basso@unimib.it (D.B.)
2 Consorzio Nazionale Interuniversitario per le Scienze del Mare—CoNISMa, Local Research Unit of Milano-Bicocca, 20126 Milan, Italy
3 Marine Protected Area "Capo Carbonara" (MPACC), Via Roma 60, 09049 Villasimius, Italy; direzione@ampcapocarbonara.it (F.A.); ambiente@ampcapocarbonara.it (N.C.)
4 Red Sea Research Center, Division of Biological and Environmental Science and Engineering, King Abdullah University of Science and Technology, Thuwal 23955-6900, Saudi Arabia; fabio.marchese@kaust.edu.sa
* Correspondence: valentina.bracchi@unimib.it

Abstract: Mediterranean rhodolith beds are priority marine benthic habitats for the European Community, because of their relevance as biodiversity hotspots and their role in the carbonate budget. Presently, Mediterranean rhodolith beds typically occur within the range of 30–75 m of water depth, generally located around islands and capes, on flat or gently sloping areas. In the framework of a collaboration between the University of Milano-Bicocca and the Marine Protected Area "Capo Carbonara" (Sardinia, Italy), video explorations and sampling collections in three selected sites revealed the occurrence of a well developed and heterogeneous rhodolith bed. This bed covers an area >41 km^2 around the cape, with live coverage ranging between 6.50 and 55.25%. Rhodoliths showed interesting morphostructural differences. They are small compact pralines at the Serpentara Island, associated with gravelly sand, or bigger boxwork at the Santa Caterina shoal associated with sand, whereas branches are reported mostly in the Is Piscadeddus shoal, associated with muddy sand. Both in the Santa Caterina shoal and the Serpentara Island, rhodoliths generally show a spheroidal shape, associated with a mean value of currents of 4.3 and 7.3 cm/s, respectively, up to a maximum of 17.7 cm/s at Serpentara, whereas in the Is Piscadeddus shoal rhodolith shape is variable and current velocity is significantly lower. The different hydrodynamic regime, with a constant current directed SW, which deviates around the cape towards E, is responsible for such morphostructural heterogeneity, with the site of the Serpentara Island being the most exposed to a constant unidirectional and strong current. We can associate current velocity with specific rhodolith morphotypes. The morphostructural definition of the heterogeneity of rhodoliths across large beds must be considered for appropriate management policies.

Keywords: rhodolith; morphotype; shape; size; heterogeneity; currents

Citation: Bracchi, V.A.; Caronni, S.; Meroni, A.N.; Burguett, E.G.; Atzori, F.; Cadoni, N.; Marchese, F.; Basso, D. Morphostructural Characterization of the Heterogeneous Rhodolith Bed at the Marine Protected Area "Capo Carbonara" (Italy) and Hydrodynamics. *Diversity* **2022**, *14*, 51. https://doi.org/10.3390/d14010051

Academic Editor: Fernando Tuya

Received: 17 December 2021
Accepted: 8 January 2022
Published: 13 January 2022

1. Introduction

Crustose Coralline Algae (CCA) are slow-growing and long-lived organisms that act as ecosystem engineers secreting high-Mg carbonate, forming both mobile (i.e., rhodoliths) and stable substrates (i.e., algal reefs). Rhodoliths are unattached nodules, mostly consisting of CCA [1], at least 50% of the total volume [2], in the form of a single or multiple coralline algal species, frequently overgrowing one over the other, and with a wide variety of growth-form, from foliose to fruticose to lumpy [3,4]. They can develop without any type of nucleus

or around skeletal or non-skeletal nuclei, usually producing a concentric arrangement of the algal thalli [5].

Three different morphotypes of rhodolith are distinguished, depending on the size, the inner structure, the external shape, the algal growth forms, and the taxonomic composition: boxwork, usually large and vacuolar; praline, compact and nodular; and branches [6]. The shape is defined as ellipsoidal, discoidal, and spheroidal [1,6,7]. Rhodolith shape can depend upon the inherited shape of the nucleus [8,9] or can be the result of species-specific growth habits and degrees of water motion [10].

Rhodolith survival depends on overturning and consequently on the possibility to continue their accretion by avoiding overgrowing by other organisms and smothering by burial [6,11–15]. Water motion, such as waves and currents, has been indicated as the main responsible for maintaining the rhodoliths unburied [16–19], and rhodoliths are often associated with sedimentary structures, such as ripple marks and dunes [19–22]. Some authors demonstrated that rhodoliths do not need to be exposed to threshold hydrodynamic forces to avoid burial [23,24], suggesting a primary role of bioturbation [23,25]. Despite this, rhodoliths are often associated with sedimentary structures, such as ripple marks and dunes [19–22].

The relation between rhodolith outer/inner structure and water energy/water depth is debated in the literature, and no straightforward interpretation can be drawn. Moreover, only qualitative indications on velocity and frequency of current related to specific shape or morphotype have been provided thus far, included both field measurements, experimental models, and tanks [6,23,24,26–28].

Rhodolith beds are formed by aggregation of free-living (>10%) rhodoliths [18,29], constituting an important biogenic marine habitat that represents an important transition between mobile and stable substrates, generally on flat or gently sloping seabed [29]. The identification of rhodolith beds, their areal distribution and vitality, their main features (morphotype, shape), and CCA species are all fundamental topics for the sustainable management of the marine environment. Their 3D structure serves as a habitat for a diverse associated community and as a local hotspot of biodiversity, providing a suite of ecosystem goods and services [29,30]. Rhodolith beds have been reported from the intertidal down to 270 m depth and are distributed worldwide [1,31,32]. Mediterranean rhodolith beds extend mainly in circalittoral detritic bottoms, while they are more scattered in the infralittoral zone [33]. In the Mediterranean Sea, they occur between 9 and 150 m [28–30], typically within 30 and 75 m of water depth [33]. These beds are presently located around islands and capes, on top of submarine plateaus, seamounts, marine terraces, channels, and banks [33,34]. Mediterranean rhodolith beds are considered as marine benthic habitats of high conservation interest and subjected to a special plan for protection within the framework of the United Nations Program's Mediterranean Action Plan [35]. They are one of the marine habitats included in the monitoring program in the Marine Strategy Framework Directive 2008/56/EC of the European Community. In the framework of an agreement between the University of Milano-Bicocca and the Marine Protected Area (MPA) "Capo Carbonara" (Villasimius, South Sardinia, Italy), a monitoring project for the Italian Marine Strategy Framework Program was conducted between 2017 and 2019 to explore the seafloor of the MPA where rhodolith occurrence was already reported [36]. Remote datasets (bathymetry and backscatter data) were already collected by the MPA and provided the basis for the sampling campaign. This work aims at the morphostructural characterization of the large and heterogeneous rhodolith bed occurring in the infra- and circalittoral zone of the MPA "Capo Carbonara", framing the morphometric features of rhodoliths and the oceanographic variables to depict the main factors driving the development and survival of this habitat. The description and characterization of the heterogeneity of rhodoliths across a bed is a key factor for the identification of appropriate and focused measures of protection and conservation of this kind of habitat.

2. Study Site

The MPA "Capo Carbonara" was established by the Ministry of 'Environment and Protection of Land and Sea, hereby MITE (Ministry of Ecological Transition), by Ministerial Decree of 15 September 1998, modified in 1999 and totally replaced by Ministerial Decree of 7 February 2012 (GU No. 113 of 16 May 2012). The MPA (14,340 hectares and four different levels of protection) is located along the SE coast of Sardinia (Italy) from Capo Boi (W) to the area in front of Serpentara Island (E), both placed in the Municipality of Villasimius (SU, Sardinia, Italy), the local management body of the MPA (Figure 1a,b). The territory of the MPA is divided into two large gulfs (Carbonara gulf to the W and Simius gulf to the E) by the granitic ridge of Capo Carbonara and Cavoli Island (Figure 1b). Capo Carbonara MPA extends seaward on the whole continental shelf, down to an average of 125 m water depth (Figure 1b). The eastern sector (Simius gulf) is characterized by a larger gently inclined shelf, except for the area of Serpentara island, whereas in the W the shelf is steeper [36]. Submerged beaches are characterized by mobile terrigenous sediment, which becomes finer from W to E [36]. The shelf is characterized by the occurrence of *Posidonia oceanica* meadows, quite continuously distributed along the MPA coast, except for Simius and Molentis channels in the Simius gulf [34]. The meadows extend up to 36 m water depth. Below this limit down to 60 m water depth, calcareous biogenic sands and pebbles (rhodoliths) occur [36], with large areas characterized by sedimentary structures, such as dunes, mega-ripples, and ripples, especially in the W sector (Carbonara gulf) [36]. Rhodoliths are indicated within troughs of such sedimentary structures [36]. Moreover, between 40 and 50 m water depth, coralligenous elongated banks are also reported. [36]. Below 60 m water depth, sediments are fine sands and mud [36].

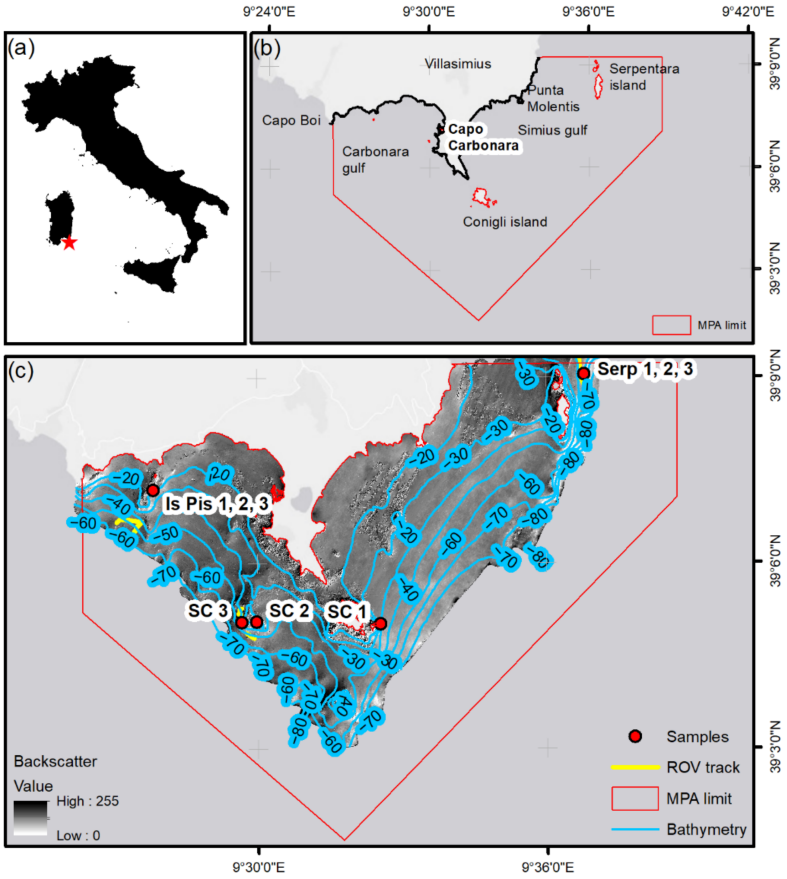

Figure 1. (**a**,**b**) geographical location of the studied area, with the indication of the MPA limit; (**c**) backscatter photomosaic of the area (property of the MPA) with the indication of the ROV tracks and sampling location. Is Pis is for Is Piscadeddus, SC is for Santa Caterina, and Serp is for Serpentara. Service layer credit in (**b**,**c**): Esri, HERE, Garmin, (C) OpenStreetMap contributors.

3. Materials and Methods

3.1. Sampling

In this study we identified 3 sites in the MPA "Capo Carbonara" at a distance of >200 m (Figure 1c, Table 1): the Is Piscadeddus shoal (from here on Is Piscadeddus) towards W, the Santa Caterina shoal (from here on Santa Caterina) in the middle, and the Serpentara Island (from here on Serpentara) towards E. Each site was investigated by a remotely operated vehicle (ROV Steelhead Seamore, property of the University of Milano-Bicocca, Milan, Italy), equipped with two cameras, to ascertain the occurrence of live rhodoliths, and to select the sites for sampling. For each site, 3 replicas were obtained. At Is Piscadeddus, samples were collected using a Van Veen Grab (1100 cm^2), whereas in the other 2 sites, samples were collected by scuba divers (Santa Caterina and Serpentara 1600 cm^2).

A pristine sample of 200 g was sub-sampled from each replica to conduct grain size analysis. Then, all the live rhodoliths were manually extracted at the time of collection from each replica.

Each rhodolith was classified *per* morphotype (Boxwork-BX, Praline-PR, and Branches-BR) following Basso [5].

BX and PR were measured (long, intermediate, and short axes (Table S1) to describe the size and the shape. Only the long axis of BR has been measured. Ternary plots *per* site were realized by using the Excel spreadsheet Triplot [37] modified from Sneed and Folk [38] to identify the most important shape *per* site. Moreover, long axis measures *per* site were expressed by boxplots to highlight differences in maximum size of rhodoliths among sites.

We calculated the coverage (cm^2 and %) of live rhodoliths *per* replica by placing them on a centimeter sheet and measuring the covered area (cm^2). We then expressed the results of coverage both in cm^2 and % with respect to the total sampled surface (Van Veen grab sampler/divers) (Table 2). Rhodolith coverages were also calculated by separating different morphotypes to obtain ternary plots of the contribution, in %, of each morphotype coverage *per* replica.

Table 1. List of samples, with the indication of the year of collection, coordinates, depth, and type of sampler.

Samples	Year	Coordinates	Depth (m)	Type
Is Piscadeddus 1	2018	39.112; 9.4518	45	Van Veen grab
Is Piscadeddus 2	2018	39.112; 9.4518		
Is Piscadeddus 3	2018	39.1074, 9.4558		
Santa Caterina 1	2017	39.0865, 9.4966	40	Scuba diver
Santa Caterina 2	2017	39.0863, 9.4964		
Santa Caterina 3	2017	39.0861, 9.4963		
Serpentara 1	2019	39.1493, 9.6124	59	Scuba diver
Serpentara 2	2019	39.1493, 9.6124		
Serpentara 3	2019	39.1493, 9.6124		

Moreover, to better evaluate and describe differences in the rhodolith size, BX and PR were subdivided into two subgroups identified upon the dimension of the long axis: greater and lesser than 2 cm. We reported the coverage of these subgroups separately (Table 2).

Table 2. Coverage of live rhodoliths and grain size analysis. Boxwork (BX) and praline (PR) have been subdivided in rhodolith with the long axis greater or lesser than 2 cm. In the first four columns, coverage is expressed in cm^2. Coverage (%) is expressed *per* morphotype (column 5), and as total (cm^2 and %, column 6) For grain size (column 7): G for gravel. S for sand, and M for mud.

Sample	BX (cm^2)		PR (cm^2)		Morphotype (%)			Rhodoliths Coverage		Grain Size (%)		
	<2 cm	>2 cm	<2 cm	>2 cm	BX	PR	BR	cm^2	%	G	S	M
Is Piscadeddus 1	0	0	19.7	34	0	70.3	29.7	76.4	6.95	11.7	72.9	15.4
Is Piscadeddus 2	0	0	24.7	26.7	0	55	45	93.5	8.50	12.3	73.5	14.2
Is Piscadeddus 3	0	0	27.4	24.6	0	72.7	27.3	71.5	6.50	7.98	76.1	16
Santa Caterina 1	0	535	135	137	60.5	30.7	8.8	884	55.25	26.5	72.4	1.12
Santa Caterina 2	0	214	45.4	347	33.2	51.7	15	642.7	40.17	29.3	70.5	0.2
Santa Caterina 3	0	201	149	240	27.8	53.8	18.4	723.48	45.22	32	67.5	0.46
Serpentara 1	0	0	109	84.8	0	87.7	12.3	220.6	13.79	35.3	59.1	5.56
Serpentara 2	0	0	297	184	0	94.6	5.4	507.9	31.74	50.7	43.7	5.57
Serpentara 3	0	0	234	113	0	78.4	21.6	442.4	27.65	36.5	57	6.52

3.2. Statistical Analysis

The coverage percentage of total live rhodoliths, the coverage area (cm^2) for every morphotype, and the grain size *per* replica were used as the main response variables. The size of rhodoliths was considered only for PR as BX. Data were analyzed by means of univariate statistical analyses using the software GMAV5 [39]. Cochran's test was run prior to each ANOVA to test for homogeneity of variances and normality was assured by the Kolmogorov–Smirnov test. Student–Newman–Keuls (SNK) tests were used for a posteriori comparison of means in case of significant ANOVA results [40]. First, one-way ANOVAs were overall run to test for differences in the total coverage percentage (%) of rhodoliths. Another two-way ANOVAs were performed to test for differences in the coverage area for pralines of different sizes among sites (3 levels, fixed: Is Piscadeddus vs. Santa Caterina vs. Serpentara) and sizes (2 levels, fixed: <2 cm vs. >2 cm for pralines). Two more two-way ANOVAs were run to highlight differences in the coverage area, respectively, among sites (3 levels, fixed: Is Piscadeddus vs. Santa Caterina vs. Serpentara) and morphotypes (3 levels, fixed: pralines vs. branches vs. boxworks). The percentage of sediment belonging to the three main size classes (mud, sand, and gravel) was considered as the main response variable, and a two-way ANOVA was run to test for differences in the percentage of sediment among sites (3 levels, fixed: Is Piscadeddus vs. Santa Caterina vs. Serpentara) and grain sizes (mud vs. sand vs. gravel).

3.3. Environmental Data

Monthly 3-dimensional oceanographic variables (temperature, salinity, and currents) were obtained from the high-resolution Mediterranean Sea Monitoring and Forecasting Centre (MFC) physical reanalysis product (MEDSEA) [41], retrieved from the E.U. Copernicus Marine Service Information platform, available at https://resources.marine.copernicus.eu/product-detail/MEDSEA_MULTIYEAR_PHY_006_004/INFORMATION (accessed on 3 December 2021). The time interval considered was 2017-2019. These data were produced by assimilating temperature, salinity, and sea level anomaly observations in numerical simulations performed with the Nucleus for European Modeling of the Ocean (NEMO) model. The model exploits a horizontal grid spacing of 1/24° (roughly 5 km), and 141 stretched vertical levels, with thickness ranging between 1 and 6 m in the upper 80 m of the ocean. As the samples were relatively close to the coastlines and the numerical model had a smoother bathymetry with respect to the real one (for numerical stability constraints), an area of roughly 25 km × 25 km centered on the sample positions was used to retrieve the average current to characterize each site. Current velocity was expressed in cm/s, whereas current

direction was expressed as counterclockwise angles with respect to the E. Temperature and salinity were retrieved pointwise using a nearest neighbor approach.

4. Results

All the three sites were characterized by the occurrence of live rhodoliths forming large coverages of the seafloor (Figure 2a–c, Table 2). Based upon these results and an already available remote dataset, we were able to map the limit of a wide area covered by rhodoliths possibly forming a unique but highly heterogenous bed around Carbonara Cape, with an extension of 41.08 km^2 (Figure 2d).

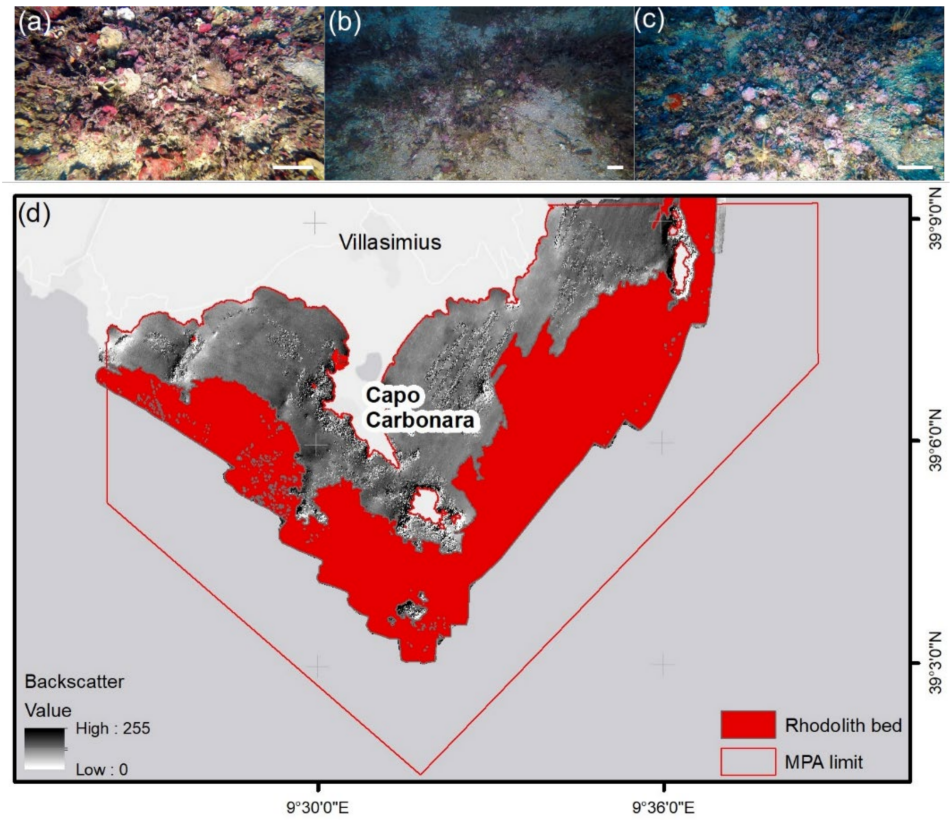

Figure 2. (**a**) Is Piscadeddus, (**b**) Santa Caterina, and (**c**) Serpentara video frames extracted from the ROV survey certifying the occurrence of a live and well-developed rhodolith bed. The scale bar indicates 5 cm. (**d**) map of the rhodolith bed in the MPA "Capo Carbonara". Service layer credit in (**d**): Esri, HERE, Garmin, (C) OpenStreetMap contributors.

4.1. Sampling

Differences in live coverage among sites were statistically significant (File S1), with Santa Caterina having the highest coverage (up to 55.25%), followed by Serpentara (up to 31.74%), and then Is Piscadeddus that had the lowest coverage (up to 6.50%) (Table 2). There was a statistically significant difference in coverage in the three studied sites among the dominant morphotypes (Figures 2a–c and 3, Table 2 and File S1. Is Piscadeddus had a similar coverage value for pralines and branches (BX (absent) < PR = BR, Table 2 and File S1). Santa Caterina was dominated by the boxworks, followed by pralines, and then branches (BX > PR > BR, Table 2 and File S1). Serpentara had mostly pralines, followed by branches and no boxwork (BX (absent) < BR < PR, Table 2 and File S1). Santa Caterina was different from the other two sites because of the unique occurrence of boxwork rhodoliths (Table 2 and File S1). The coverage of pralines was similar between Santa Caterina and Serpentara (Table 2 and File S1). Branches were identified in all three sites, but they were

considerably abundant, in terms of coverage, only in Is Piscadeddus (Figure 3, Table 2 and File S1).

Rhodolith size was not constant (Figure 4, Table S1). At Is Piscadeddus, pralines (only 12 specimens) showed a wide range (max: 7.1 × 6.4 × 1.6 cm, Figure 4, Tables 2 and S1), whereas branches usually had a diameter <1.5 cm. At Santa Caterina, all the boxworks and pralines were >2 cm (max: 9.9 × 7.8 × 4.5 cm, Figure 4, Table S1). Moreover, in Santa Caterina long axis of pralines was mostly between 3 and 4 cm, whereas the long axis of boxwork was between 4 and 7 cm (Figure 4, Table S1). Serpentara was characterized by >2 cm pralines (max: 4.5 × 2.8 × 1.5 cm, Figure 4, Table S1). The long axis of pralines was mostly between 2 and 3 cm (Figure 4). Both in Santa Caterina and Serpentara, branches were present and showed a diameter ranging from 1 to 4 cm.

Statistical analysis on the relation between site and praline dimension supports the distinction of Santa Caterina because of the occurrence of bigger pralines than in Serpentara (File S1).

Figure 5 shows the ternary plots of the boxwork and praline shapes. Is Piscadeddus was characterized by a very low number of specimens (only 12 pralines), and the shape of these rhodoliths was variable, not corresponding to a specific category (Figure 5a). Both Santa Caterina (Figure 5b) and Serpentara (Figure 5c) were dominated by spheroidal rhodoliths (Santa Caterina = 81 specimens: Serpentara = 90 specimens, Figure 5d). In both sites, discoidal (Santa Caterina = 9 specimens: Serpentara = 7 specimens), and ellipsoidal (Santa Caterina = 4 specimens: Serpentara = 2 specimens) or the combination of the two (Santa Caterina = 19 specimens: Serpentara = 914specimens) rhodoliths were reported (Figure 5b–d).

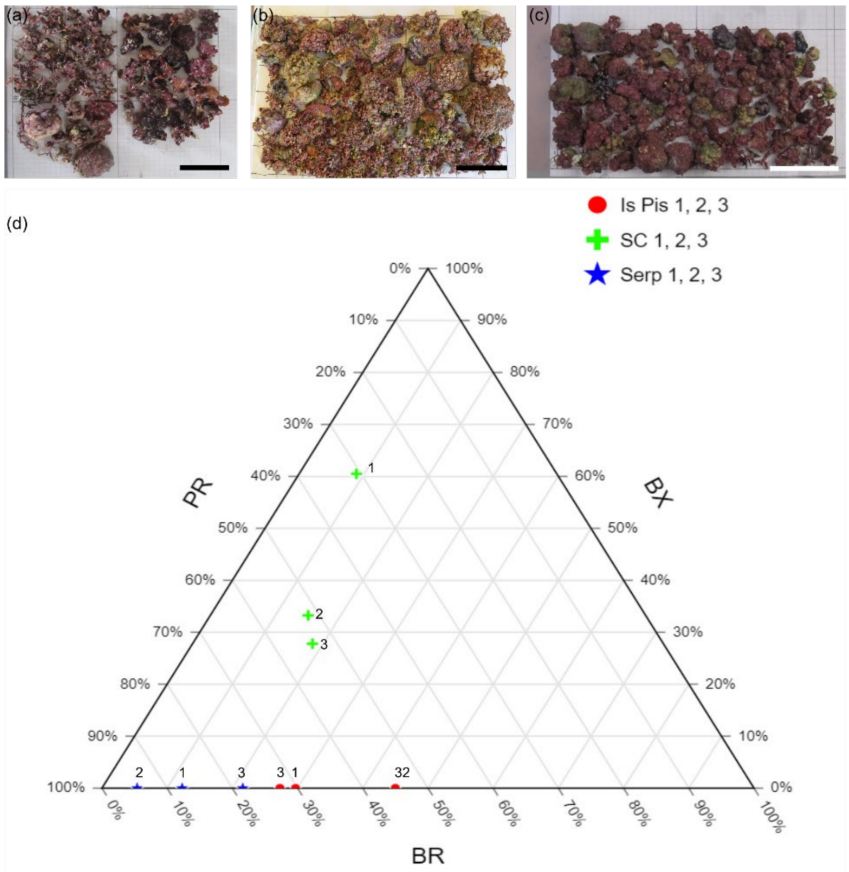

Figure 3. (**a**) Is Piscadeddus 1, (**b**) Santa Caterina 2, and (**c**) Serpentara 3 replicas of live rhodoliths. Scale bar indicates 5 cm. (**d**) ternary plot of the three main morphotypes (coverage in %) per site. Is Pis is for Is Piscadeddus, SC is for Santa Caterina, and Serp is for Serpentara.

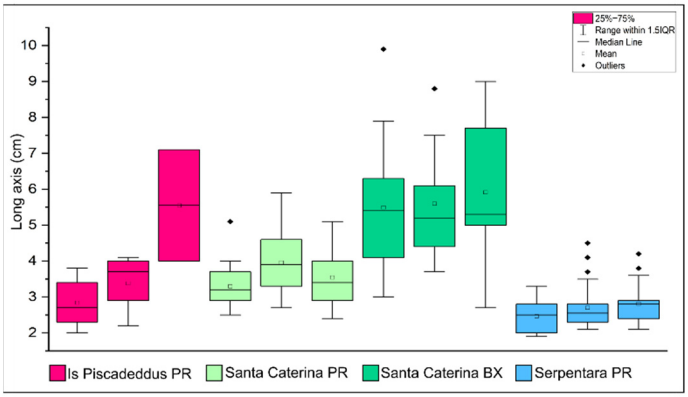

Figure 4. Boxplots of the dimension of the long axis of measured rhodoliths. PR is for praline, BX is for boxwork. Is Piscadeddus in pink, Santa Caterina PR in light green, Santa Caterina BX in green, and Serpentara PR in blue.

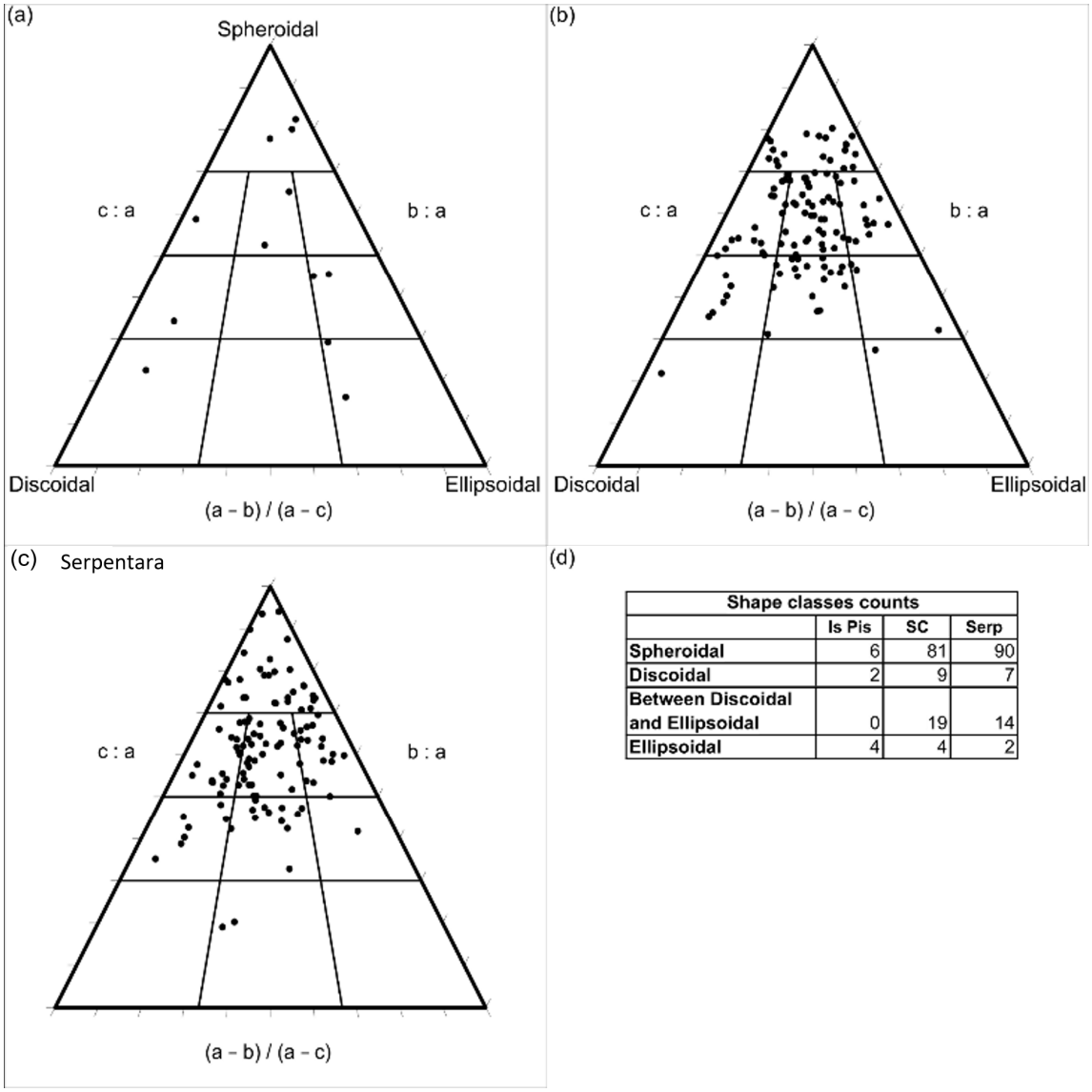

Shape classes counts			
	Is Pis	SC	Serp
Spheroidal	6	81	90
Discoidal	2	9	7
Between Discoidal and Ellipsoidal	0	19	14
Ellipsoidal	4	4	2

Figure 5. (**a**) Is Piscadeddus, (**b**) Santa Caterina, and (**c**) Serpentara ternary plots of boxwork and praline shape: a = long axis, b = intermediate axis, and c = short axis. (**d**) counting the number of specimens per shape. Is Pis is for Is Piscadeddus, SC for Santa Caterina and Serp for Serpentara.

Sand characterized all three sites, but with statistically significant differences of gravel (mostly abundant in Serpentara) and mud percentages (relatively more abundant in Is Piscadeddus) (Table 2 and File S1).

4.2. Environmental Data

The three studied sites were characterized by similar temperature and salinity ranges (Table 3, Figures S1 and S2).

Table 3. Minimum and maximum values (between 2017 and 2019) of monthly three-dimensional oceanographic variables from the high-resolution Mediterranean Sea MFC physical reanalysis product (MEDSEA) [39], retrieved from the E.U. Copernicus Marine Service Information platform, available at https://resources.marine.copernicus.eu/product-detail/MEDSEA_MULTIYEAR_PHY_006_004/INFORMATION (last accessed: 3 December 2021). In brackets is the indication of the month (from 1 = January to 12 = December). PSU = Practical Salinity Units.

Sites	T (°C)		Salinity (psu)		Current Velocity (cm/s)		
	Max	Min	Max	Min	Max	Min	Mean
Is Piscadeddus	19.9	13.9	38.5	37.9	7.3	0.7	3.1
Santa Caterina	21.1	13.9	38.5	37.9	9.9	0.7	4.3
Serpentara	17.5	13.9	38.5	37.9	17.7	1.2	7.3

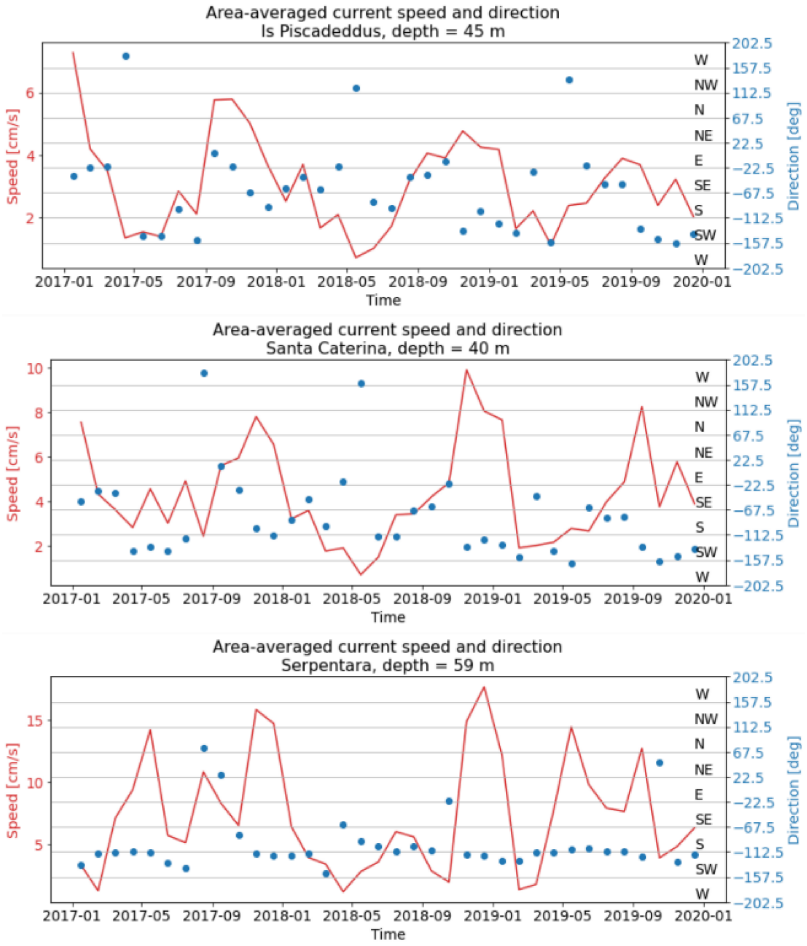

Figure 6. Monthly horizontal current (direction and velocity) obtained from the high-resolution Mediterranean Sea MFC physical reanalysis product (MEDSEA) [39], retrieved from the E.U. Copernicus Marine Service Information platform, available at https://resources.marine.copernicus.eu/product-detail/MEDSEA_MULTIYEAR_PHY_006_004/INFORMATION (accessed on 3 December 2021).

Interestingly, the bottom current direction and velocity showed the main differences among sites (Table 3, Figure 6). Velocity ranged between 0.7 and 7.3 cm/s in Is Piscadeddus, 0.7 and 9.8 in Santa Caterina, and 1.2 and 17.7 cm/s in Serpentara (Figure 6, Table 3), with a mean velocity ranging between 3.1 (Is Piscadeddus) and 7.3 (Serpentara) (Figure 6, Table 3). At Serpentara, the current was mostly directed SW, whereas both in Is Piscadeddus and in Santa Caterina it showed a more variable direction (Figure 6). Monthly maps of ocean currents between 2017 and 2019 (Figure 7) showed that a dominant current, between 10 and 17 cm/s in velocity and generally directed S-SW, characterized the eastern side of Capo Carbonara (Figure 7a,b). This current, passing the Carbonara cape, often deviated slightly westward, generating a weaker closed anticyclonic loop current to the W of Capo Carbonara (Figure 7a,b). Such a closed-loop current sometimes was not present, as shown in panels (c) and (d). This kind of configurations was rare in the time frame considered (2017–2019) and apparently did not show any link with the seasonality.

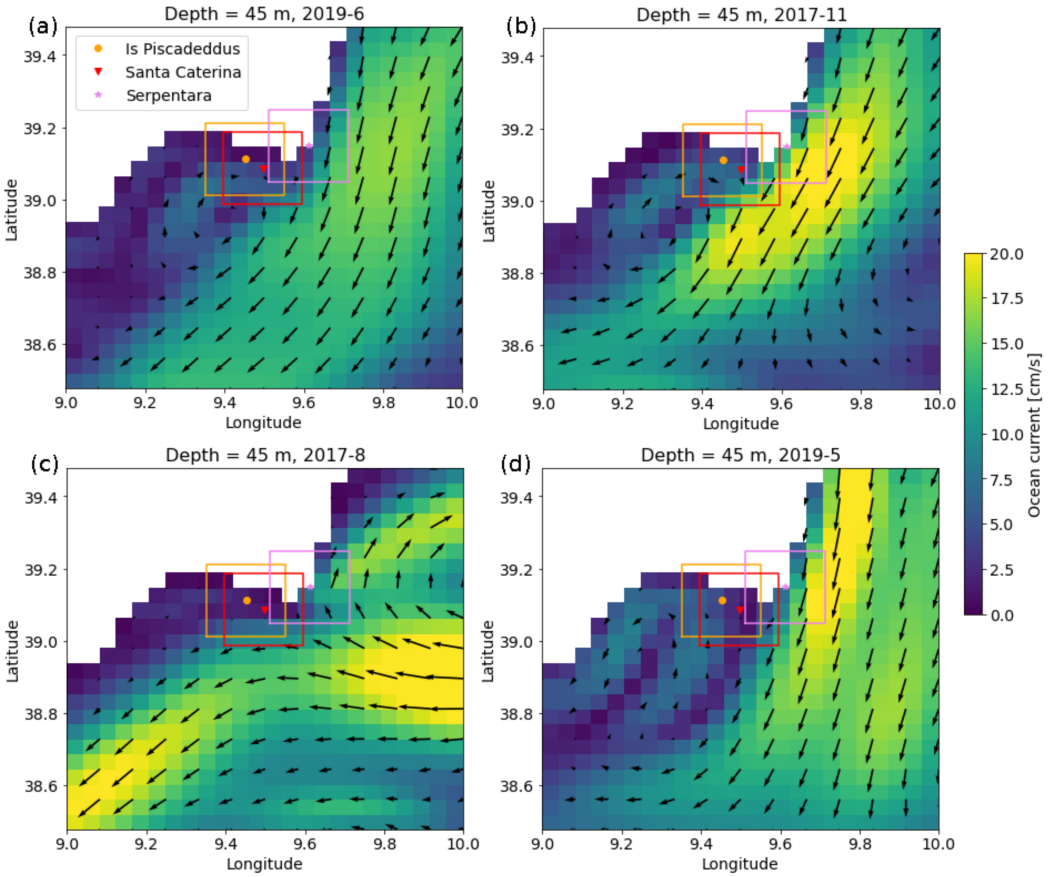

Figure 7. Example of the maps of monthly mean currents at 45 m depth from the MEDSEA reanalysis product. (**a**,**b**) show a dominant current (10–15 cm/s, directed S-SW), characterizing the eastern side of Capo Carbonara and deviating westward, generating a weaker closed anticyclonic loop current to the W. (**c**,**d**) are examples of the rare configuration of the local circulation with no anticyclonic loop.

5. Discussion

This study confirms the existence of a large and well-developed rhodolith bed in the territory of the MPA "Capo Carbonara" (Figure 2), with a coverage raging between 6.50 and 55.25% (Table 2). Is Piscadeddus shows the lowest values, but the observation conducted by ROV (Figure 2a) indicates that in Is Piscadeddus the inherent randomness of the sampling possibly underestimated the abundance of rhodoliths.

The heterogeneity is firstly due to the morphostructural variation of rhodoliths around the Carbonara cape. The Is Piscadeddus shoal is the westernmost site, and it is placed very next to the shoreline, at 45 m water depth, in a sheltered location (Figure 1c). The

rhodoliths are sparser, both thin unattached branches and rare praline that are not characterized by a specific shape (Figures 2–5). Associated sediment is a muddy sand (Table 2), which is consistent with the low and inconstant (non-unidirectional) hydrodynamic regime (Figures 6 and 7, Table 3). The low live coverage and the variable praline shapes suggest that this part of the bed is under unfavorable conditions for its development. Burial is detrimental for rhodolith survival [11–15], and the occurrence of mud suggests that these rhodoliths possibly undergo periodical burial by sediments.

Both Santa Caterina and Serpentara sites show a well-developed bed with high percentage of live coverage, although the rhodoliths have significant differences in morphotype, shape and dimension (Figures 3–5, Tables 2 and 3 and File S1). Santa Caterina is placed in the central zone of the MPA at 40 m water depth (Figure 1c). This site is characterized by very large boxwork and praline rhodoliths with a prevalent spheroidal shape (Figures 2–5). Interestingly, branches are usually thick. The associated sediments are coarse sands (Table 2). Serpentara is the easternmost site, at 60 m water depth (Figure 1c), and in this site rhodoliths are mostly compact spheroidal pralines (Figures 2–5), with a mean long axis ranging between 2 and 3 cm (Figure 4). These rhodoliths are associated with gravelly sand (Table 2). These results firstly underline that, although in MPA "Capo Carbonara" we identified a unique rhodolith bed, there is a strong morphostructural heterogeneity, as typical for some other Mediterranean rhodoliths beds [42,43]. The morphometrics definition of rhodoliths based on the quantitative description of morphotype and shape easily depicts such heterogeneity and surely represents the first and mandatory step for the evaluation of the variability of this kind of habitat, as suggested by Basso et al. [29].

No straightforward interpretation exists on the relation between the rhodolith shape [1,7], morphotype [6,16,44], and size [10,14,45–48] with respect to the water energy and depth. Due to the evident heterogeneity of the rhodoliths across the studied bed, in a relatively similar bathymetric interval (45–60 m water depth), we focused our attention on the identification of possible environmental variables as drivers for such diversity.

Salinity and temperature are quite constant across the MPA (Table 3, Figures S1 and S2) and, therefore, cannot be the factors underlying differences in the rhodoliths shape, size, and morphotype. As expected, the most variable environmental parameter is the hydrodynamic regime, and this work links specific combinations of shape/morphotype/size to specific values of current velocity and associated grain size. Serpentara site records the most energetic regime with a quite constant unidirectional current (SW-directed) with a velocity ranging between 1.2 and 17.7 cm/s and a mean of 7.3 cm/s (Figures 6 and 7, Table 3). On the contrary, both Santa Caterina and Is Piscadeddus sites are characterized by a generally low current velocity that is not unidirectional during the time interval considered for this study (Figures 6 and 7, Table 3). The dominant current, SW-directed in the studied area, often deviates slightly westward passing the Carbonara cape, generating a weaker, closed anticyclonic loop current to the W of the cape (Figure 7a,b). In rare periods, this loop does not appear (Figure 7c,d). This firstly suggests that currents might be determined by some large-scale features of the Tyrrhenian Sea, whose characterization goes beyond the scope of the present study. In the studied sites, the differences in current velocity and direction translate in morphostructural diversification of rhodoliths across the bed, generating such heterogeneity.

These observations partially match with previous literature. Basso [5] firstly discussed the distribution of different rhodolith morphotypes in the framework of the Mediterranean benthic zonation. The author suggested that frequent overturning under high water energy generates compact pralines, generally in shallow water. On the contrary, more stable facies can undergo burial under high sedimentation rates, or alternatively, in case of low sedimentation rate, neighboring rhodoliths can coalesce and generate a rigid, highly porous, more stable framework (boxwork and then coralligenous), this generally in deeper settings. As expected from this predictive scheme, small, compacted pralines characterize Serpentara site, which experienced the highest and more constant hydrodynamic regime, although being the deepest site, whereas in Santa Caterina boxwork and bigger pralines are dominant.

Moreover, pralines generally show a compact and small structure with no voids [7,21,49], such as the rhodoliths in Serpentara. In Santa Caterina instead, the dominance of boxwork is consistent with a lower hydrodynamic regime [7,21,49] even if under a low sedimentation rate [7].

Our results show that around Carbonara cape, intermediate energy generates the largest rhodoliths, as suggested by Amado Fihlo et al. [47] and Gagnon et al. [48], and in contradiction with some other authors [10,14,45,46]. Where hydrodynamic regime is too low, rhodoliths are less abundant (Is Piscadeddus), whereas, in the most energetic regime, rhodoliths are well developed but with small and compact structures (Serpentara) [7]. Branches occurring in all three sites do not contribute to the definition of such heterogeneity. Finally, our findings also suggest that the bathymetry cannot be considered as a discriminant for rhodolith shape, size, and morphotype. Rather it is a specific and local combination of current direction, current velocity, and seafloor geomorphology that drives the morphostructural heterogeneity of rhodoliths.

In this study, we focused on the morphometric definition of live rhodoliths as a direct measure and expression of the heterogeneity of rhodolith beds. We demonstrated that, with this kind of approach, it is possible to easily identify zones of the rhodolith bed characterized by the highest conservation values and providing a powerful tool to manage in an appropriate way large seafloor area interested by the occurrence of live rhodoliths. As suggested by other authors [10], such heterogeneity also translates into differences in the algal community and the genera/species distribution, which may be future interesting studies on these samples.

6. Conclusions

The rhodolith bed in the territory of the MPA "Capo Carbonara" (Italy) has been mapped, covering an area of more than 41 km^2. Live rhodoliths have a variable coverage, ranging between 6.50% at the Is Piscadeddus shoal, up to 55.25% at the Santa Caterina shoal.

This rhodolith bed shows strong morphostructural heterogeneity. At Is Piscadeddus, they are sparser, branch-dominated, with rare praline, and associated with muddy sand. At Santa Caterina, rhodoliths are generally boxwork and pralines, large and with a spheroidal shape and associated with sand. At Serpentara, pralines are dominant but usually with a small spheroidal shape (long axis ranging between 2 and 3 cm) and associated with gravelly sand.

The different hydrodynamic regime around the cape supports such heterogeneity, being Serpentara site under a more constant (SW directed) and strongest (mean velocity current 7.3 cm/s) hydrodynamic regime, which translates in small spheroidal praline according to Basso [5]. Santa Caterina has an intermediate hydrodynamic regime, and rhodoliths generally have bigger sizes as the results of a long-lasting development of such rhodoliths in a more stable condition. At Is Piscadeddus, the low hydrodynamic regime is responsible for the mud abundance in the associated sediments, which makes the rhodolith' survival difficult because of possible periodical sediment burial.

The heterogeneity of the rhodolith bed of the MPA "Capo Carbonara" has been described based upon the morphostructural characterization and quantification of live rhodoliths coverage, morphotypes, and shapes. The identification of such heterogeneity, above all in large rhodolith beds, is crucial for the appropriate identification of seabed areas with the highest conservation values and for the marine spatial planning management policy aimed at the conservation of this kind of habitat.

Supplementary Materials: The following are available online at https://www.mdpi.com/article/10.3390/d14010051/s1, Figure S1: Monthly three-dimensional temperature obtained from the high-resolution Mediterranean Sea Monitoring and Forecasting Centre (MFC) physical reanalysis product (MEDSEA) [33], retrieved from the E.U. Copernicus Marine Service Information platform, available at https://resources.marine.copernicus.eu/product-detail/MEDSEA_MULTIYEAR_PHY_006_004/INFORMATION (accessed on 3 December 2021). Figure S2: Monthly three-dimensional salinity obtained from the high-resolution Mediterranean Sea MFC physical reanalysis product

(MEDSEA) [33], retrieved from the E.U. Copernicus Marine Service Information platform, available at https://resources.marine.copernicus.eu/product-detail/MEDSEA_MULTIYEAR_PHY_006_004/INFORMATION (accessed on 3 December 2021). Table S1: Measures of the long, intermediate, and short axes of boxwork and praline rhodoliths of the three studied sites. File S1: Results of the ANOVAand SNK tests.

Author Contributions: Conceptualization, V.A.B. and D.B.; methodology, V.A.B., D.B., A.N.M. and S.C; formal analysis, V.A.B., E.G.B., A.N.M., S.C.; investigation, V.A.B., D.B., N.C., F.M., E.G.B.; resources, F.A. and D.B.; data curation, V.A.B., S.C., A.N.M. and D.B; writing—original draft preparation, V.A.B.; writing—review and editing, V.A.B., A.N.M., F.A. and D.B.; supervision, D.B.; project administration, D.B. and F.A.; funding acquisition, D.B. and F.A. All authors have read and agreed to the published version of the manuscript.

Funding: This research was funded in the framework of the agreement between the University of Milano-Bicocca and the Marine Protected area of Capo Carbonara "Convenzione Operativa tra L'area Marina Protetta "Capo Carbonara" e L'universita degli Studi di Milano Bicocca per la Realizzazione delle Attività di Monitoraggio e Ricerca Sulla Strategia Marina", grant number 2017-CONV25-0092.

Institutional Review Board Statement: Not applicable.

Informed Consent Statement: Not applicable.

Data Availability Statement: Not applicable.

Acknowledgments: We thank the associate Editor Fernando Tuya, together with Juan Carlos Braga and another anonymous reviewer for their helpful suggestions during the first revision of the manuscript. This article is a contribution to the Project MIUR-Dipartimenti di Eccellenza 2018–2022 DISAT-UNIMIB.

Conflicts of Interest: The authors declare no conflict of interest.

References

1. Bosence, D.W.J. Description and classification of rhodoliths (rhodoids, rhodolites). In *Coated Grains*; Peryt, T.M., Ed.; Springer: Berlin/Heidelberg, Germany, 1983; pp. 217–224.
2. Steneck, R.S. The ecology of coralline algae crusts: Convergent patterns and adaptive strategies. *Ann. Rev. Ecol. Syst.* **1986**, *17*, 273–303. [CrossRef]
3. Bosence, D.W.J. The occurrence and ecology of recent rhodoliths—A review. In *Coated Grains*; Peryt, T.M., Ed.; Springer: Berlin/Heidelberg, Germany, 1983; pp. 225–242.
4. Woelkerling, J.; Irvine, L.M.; Harvey, A.S. Growth forms in non-geniculate coralline red algae (Corallinales, Rhodophyta). *Aust. Syst. Bot.* **1993**, *6*, 277–293. [CrossRef]
5. Freiwald, A.; Henrich, R. Reefal coralline algal build-ups within the Arctic Circle: Morphology and sedimentary dynamics under extreme environmental seasonality. *Sedimentology* **1994**, *41*, 963–984. [CrossRef]
6. Bosence, D.W.J. Ecological studies on two unattached coralline algae from Western Ireland. *Palaeontology* **1976**, *19*, 365–395.
7. Basso, D. Deep rhodolith distribution in the Pontian Islands, Italy: A model for the paleoecology of a temperate sea. *Palaeogeogr. Palaeoclimatol. Palaeoecol.* **1998**, *137*, 173–187. [CrossRef]
8. Braga, J.C.; Martín, J.M. Neogene coralline-algal growth-forms and their palaeoenvironments in the Almanzora River Valley (Almeria, S.E. Spain). *Palaeogeogr. Palaeoclimatol. Palaeoecol.* **1988**, *67*, 285–303. [CrossRef]
9. Aguirre, J.; Braga, J.C.; Martín, J.M. Algal nodules in the upper Pliocene deposits at the coast of Cadiz (S Spain). *Boll. Soc. Paleontol. Ital.* **1993**, *1*, 1–7.
10. Steller, D.L.; Foster, M.S. Environmental factors influencing distribution and morphology of rhodoliths on Bahía Concepción, B.CS, México. *J. Exp. Mar. Biol. Ecol.* **1995**, *194*, 201–212. [CrossRef]
11. BIOMAERL Team. Conservation and management of northeast Atlantic and Mediterranean maërl beds. *Aquat. Conserv. Mar. Freshw. Ecosyst.* **2003**, *13*, S65–S76. [CrossRef]
12. Bordehore, C.; Borg, J.A.; Lanfranco, E.; Ramos-Esplá, A.A.; Rizzo, F.; Schembri, P.J. Trawling as a major threat to Mediterranean maërl beds. Proceedings of the First Mediterranean symposium on Marine Vegetation, Ajaccio. *Mednature* **2002**, *1*, 105–109.
13. Bordehore, C.; Ramos-Esplá, A.A.; Riosmena-Rodríguez, R. Comparative study of two maërl beds with different otter trawling history, southeast Iberian Peninsula. *Aquat. Conserv. Mar. Freshw. Ecosyst.* **2003**, *13*, S43–S54. [CrossRef]
14. Bahia, R.G.; Abrantes, D.P.; Brasileiro, P.S.; Pereira-Filho, G.H.; Amado-Filho, G.M. Rhodolith bed structure along a depth gradient on the northern coast of Bahia State, Brazil. *Braz. J. Oceanog.* **2010**, *58*, 323–337. [CrossRef]
15. Riul, P.; Targino, C.H.; Farias, J.D.N.; Visscher, P.T.; Horta, P.A. Decrease of *Lithothamnion* sp. (Rhodophyta) primary production due to the deposition of a thin sediment layer. *J. Mar. Biol. Ass. UK* **2008**, *88*, 17–19.

16. Bosellini, A.; Ginsburg, R.N. Form and internal structure of recent algal nodules (rhodolites), Bermuda. *J. Geol.* **1971**, *79*, 669–682. [CrossRef]
17. Foster, M.S.; Riosmena-Rodríguez, R.; Steller, D.L.; Woelkerling, W.J. Living rhodolith beds in the Gulf of California and their implications for paleoenvironmental interpretation. *Geol. Soc. Am. Bull.* **1997**, *318*, 127–139.
18. Steller, D.L.; Riosmena-Rodríguez, R.; Foster, M.S.; Roberts, C.A. Rhodolith bed diversity in the Gulf of California: The importance of rhodolith structure and consequences of disturbance. *Aquat. Conserv. Mar. Freshw. Ecosyst.* **2003**, *13*, S5–S20. [CrossRef]
19. Barberá, C.; Moranta, J.; Ordines, F.; Ramón, M.; de Mesa, A.; Díaz-Valdés, M.; Grau, A.M.; Massutí, E. Biodiversity and habitat mapping of Menorca Channel (western Mediterranean): Implications for conservation. *Biodivers. Conserv.* **2012**, *21*, 701–728. [CrossRef]
20. Micallef, A.; Le Bas, T.; Huvenne, V.A.I.; Blondel, P.; Huhnerbach, V.; Deidun, A. A multi-method approach for benthic habitat mapping of shallow coastal areas with high-resolution multibeam data. *Cont. Shelf Res.* **2012**, *39*, 14–26. [CrossRef]
21. Sañé, E.; Chiocci, F.L.; Basso, D.; Martorelli, E. Environmental factors controlling the distribution of rhodoliths: An integrated study based on seafloor sampling, ROV and side scan sonar data, offshore the W-Pontine Archipelago. *Cont. Shelf Res.* **2016**, *129*, 10–22. [CrossRef]
22. Bracchi, V.A.; Angeletti, L.; Marchese, F.; Taviani, M.; Cardone, F.; Hajdas, I.; Grande, V.; Prampolini, M.; Caragnano, A.; Corselli, C.; et al. A resilient deep-water rhodolith bed off the Egadi Archipelago (Mediterranean Sea) and its actual paleontological significance. *Alp. Mediterr. Quat.* **2019**, *32*, 1–20.
23. Millar, K.R.; Gagnon, P. Mechanisms of stability of rhodolith beds: Sedimentological aspects. *Mar. Ecol. Prog. Ser.* **2018**, *594*, 65–83. [CrossRef]
24. O'connell, L.G.; James, N.P.; Harvey, A.S.; Luick, J.; Bone, Y.; Shepherd, S.A. Reevaluation of the inferred relationship between living rhodolith morphologies, their movement, and water energy: Implications for interpreting palaeoceanographic conditions. *Palaios* **2021**, *35*, 543–556. [CrossRef]
25. Marrack, E.C. The relationship between water motion and living rhodolith beds in the southwestern Gulf of California, Mexico. *Palaios* **1999**, *14*, 159–171. [CrossRef]
26. Basso, D.; Tomaselli, V. Paleoecological potentiality of rhodoliths: A Mediterranean case history. *Bollettino Soc. Paleontol. Ital.* **1994**, *2*, 17–27.
27. Harris, P.T.; Tsuji, Y.; Marshall, J.F.; Davies, P.J.; Honda, N.; Matsuda, H. Sand and rhodolith-gravel entrainment on the mid- to outer-shelf under a western boundary current: Fraser Island continental shelf, eastern Australia. *Mar. Geol.* **1996**, *129*, 313–330. [CrossRef]
28. Basso, D.; Nalin, R.; Campbell, S.N. Shallow-water *Sporolithon* rhodoliths from north island (New Zealand). *Palaios* **2009**, *24*, 92–103. [CrossRef]
29. Basso, D.; Babbini, L.; Kaleb, S.; Bracchi, V.; Falace, A. Monitoring deep Mediterranean rhodolith beds. *Aquat. Conserv. Mar. Freshw. Ecosyst.* **2015**, *26*, 549–561. [CrossRef]
30. Aguilar, R.; Pastor, X.; de la Torriente, A.; García, S. Deep-sea coralligenous beds observed with ROV on four seamounts in the Western Mediterranean. In *UNEP—MAP—RAC/SPA, Proceedings of the 1st Mediterranean Symposium on the Conservation of the Coralligenous and Other Calcareous Bio-Concretions, Tabarka, Tunisia, 15–16 January 2009*; Pergent-Martini, C., Brichet, M., Eds.; CAR/ASP Publishing: Tabarka, Tunisia, 2009; pp. 148–150.
31. Riosmena-Rodríguez, R. Natural history of Rhodolith/Maërl beds: Their role in near-shore biodiversity and management. In *Rhodolith/Maërl Beds: A Global Perspective*; Riosmena-Rodríguez, R., Nelson, W., Aguirre, J., Eds.; Coastal Research Library; Springer International Publishing: Cham, Switzerland, 2017; Volume 15, pp. 3–26.
32. Foster, M.S. Rhodoliths: Between rocks and soft places. *J. Phycol.* **2001**, *37*, 659–667. [CrossRef]
33. Foster, M.S.; Amado Filho, G.M.; Kamenos, K.A.; Riosmena-Rodríguez, R.; Steller, D.L. Rhodoliths and rhodolith beds. In *Research and Discoveries: The Revolution of Science Through SCUBA*; American Academy of Underwater Sciences: Mobile, AL, USA, 2013; pp. 143–155.
34. Basso, D.; Babbini, L.; Ramos-Esplá, A.A.; Salomidi, M. Mediterranean rhodolith beds. In *Rhodolith/Maërl Beds: A Global Perspective*; Riosmena-Rodríguez, R., Nelson, W., Aguirre, J., Eds.; Coastal Research Library; Springer: Cham, Switzerland, 2017; Volume 15, pp. 281–298.
35. UNEP-MAP-RAC/SPA. *Action Plan for the Conservation of the Coralligenous and Other Calcareous Bio-Concretions in the Mediterranean Sea*; Pergent-Martini, C., Brichet, M., Eds.; RAC/SPA: Tunis, Tunisia, 2008; 21p.
36. Orrù, P.; Cocco, A.; Panizza, V. Subaqueous geomorphological investigations from Capo Boi to Is Cappuccinus (south-eastern Sardinia). *Mem. Descr. Carta Geol. d'Ital.* **1994**, *LII*, 163–176.
37. Graham, D.J.; Midgley, N.G. Graphical representation of particle shape using triangular diagrams: An Excel spreadsheet method. *Earth Surf. Proc. Landf.* **2000**, *25*, 1473–1477. [CrossRef]
38. Sneed, E.D.; Folk, R.L. Pebbles in the lower Colorado river, Texas. A study in particle morphogenesis. *J. Geol.* **1958**, *66*, 114–150. [CrossRef]
39. Underwood, A.J.; Chapman, M.G.; Richards, S.A. *GMAV-5 for Windows. An Analysis of Variance Programme*; University of Sydney: Sidney, Australia, 2002.
40. Underwood, A.J. *Experiments in Ecology: Their Logical Design and Interpretation Using Analysis of Variance*; Cambridge University Express: Cambridge, UK, 1997; Volume 117, p. 524.

41. Escudier, R.; Clementi, E.; Omar, M.; Cipollone, A.; Pistoia, J.; Aydogdu, A.; Drudi, M.; Grandi, A.; Lyubartsev, V.; Lecci, R.; et al. *Mediterranean Sea Physical Reanalysis (CMEMS MED-Currents) (Version 1) Set*; Copernicus Monitoring Environment Marine Service (CMEMS): Toulouse, France, 2020.
42. Chimienti, G.; Rizzo, L.; Kaleb, S.; Falace, A.; Fraschetti, S.; Giosa, F.D.; Tursi, A.; Barbone, E.; Ungaro, N.; Mastrototaro, F. Rhodolith Beds Heterogeneity along the Apulian Continental Shelf (Mediterranean Sea). *J. Mar. Sci. Eng.* **2020**, *8*, 813. [CrossRef]
43. Rendina, F.; Kaleb, S.; Caragnano, A.; Ferrigno, F.; Appolloni, L.; Donnarumma, L.; Russo, G.F.; Sandulli, R.; Roviello, V.; Falace, A. Distribution and Characterization of Deep Rhodolith Beds off the Campania coast (SW Italy, Mediterranean Sea). *Plants* **2020**, *9*, 985. [CrossRef] [PubMed]
44. Adey, W.H.; Macintyre, I.G. Crustose coralline algae: A re-evaluation in the geological sciences. *Geol. Soc. Am. Bull.* **1973**, *84*, 883–904. [CrossRef]
45. Littler, M.M.; Littler, D.S.; Hanisak, M.D. Deep-water rhodolith distribution, productivity and growth history at sites of formation and subsequent degradation. *J. Mar. Biol. Ecol.* **1991**, *150*, 163–182. [CrossRef]
46. Riul, P.; Lacouth, P.; Pagliosa, P.R.; Christoffersen, M.L.; Horta, P. Rhodolith beds at the Easter- most extreme of South America: Community structure on an endangered environment. *Aquat. Bot.* **2009**, *90*, 315–320. [CrossRef]
47. Amado-Filho, G.M.; Maneveldt, G.; Manso, R.C.C.; Marins-Rosa, B.V.; Pacheco, M.R.; Guimarães, S.M.P.B. Structure of rhodolith beds from 4 to 55 m deep along the southern coast of Espírito Santo State, Brazil. *Cienc. Mar.* **2007**, *33*, 399–410. [CrossRef]
48. Gagnon, P.; Matheson, K.; Stapleton, M. Variation in rhodolith morphology and biogenic potential of newly discovered rhodolith beds in Newfoundland and Labrador (Canada). *Bot. Mar.* **2012**, *55*, 85–99. [CrossRef]
49. Minnery, G.A.; Rezak, R.; Bright, T.J. Depth zonation and growth form of crustose coralline algae: Flower Garden Banks, northwestern Gulf of Mexico. In *Paleoalgology: Contemporary Research and Applications*; Toomey, D.F., Nitecki, M.H., Eds.; Springer: Berlin, Germany, 1985; pp. 237–247.